Intrinsic localized modes in the charge-transfer solid PtCl

1999 J. Phys.: Condens. Matter 11 L415

(http://iopscience.iop.org/0953-8984/11/39/101)

J. Phys.: Condens. Matter **11** (1999) L415–L422. Printed in the UK PII: S0953-8984(99)06481-4

LETTER TO THE EDITOR

Intrinsic localized modes in the charge-transfer solid PtCl

K Kladko†, J Malek‡ and A R Bishop†

† Theoretical Division and Center for Nonlinear Studies, Los Alamos National Laboratory, Los Alamos, NM 87545, USA
‡ Institute of Physics, Na Slovance 2, 18221 Prague 8, Czech Republic

Received 30 July 1999

Abstract. We report a theoretical analysis of intrinsic localized modes in a quasi-one-dimensional charge-transfer solid, $[Pt(en)_2][Pt(en)_2Cl_2](ClO_4)_4$(PtCl). We discuss strongly non-linear features of resonant Raman overtone scattering measurements on PtCl, arising from quantum intrinsic localized (multiphonon) modes (ILMs) and ILM-plus-phonon states. We show that Raman scattering data display clear signs of a non-thermalization of the lattice degrees of freedom, manifested in a non-equilibrium density of intrinsic localized modes. Adiabatic lattice dynamics is used in a model two-band Peierls–Hubbard Hamiltonian, including a screened Coulomb interaction between neighbouring sites. The Hamiltonian is diagonalized on a finite chain. The calculated adiabatic potential for Peierls distortion of the Cl sublattice displays characteristic non-analytic points, related to a lattice-distortion-induced charge transfer. Possible non-adiabatic effects on ILMs are discussed.

In this letter we discuss intrinsic localized modes, i.e. multi-quanta bound states [1], in a halogen-bridged mixed-valence transition metal complex $[Pt(en)_2][Pt(en)_2Cl_2](ClO_4)_4$ (en = ethylenediamine), subsequently denoted as PtCl (see [2] and references therein). PtCl is a representative of a family of MX-chain compounds, where M stands for a transition metal (e.g., Pt, Pd, or Ni) in a mixed-valence (i.e. charge-disproportionated) state and X is a halogen (Cl, Br, or I). PtCl consists of a three-dimensional crystalline array of charged linear chains of alternating metal (Pt^{3+}) and halogen (Cl^-) ions, with $(en)_2$ ligands attached to the metals. There are also two ClO_4^- ions per unit cell to maintain charge neutrality. The structure of PtCl is given in figure 1 of [3]. Each Cl ion has two electrons in the filled p_z orbital (z is oriented along the chain axis). Pt ions have on average one electron in each d_{z^2} orbital. There are, therefore, three valence electrons or one hole per unit cell. The ground state of PtCl displays a very strong charge-density-wave (CDW) structure. Holes are redistributed to produce an alternating sequence of nominally Pt^{2+} and Pt^{4+} ions that have nearly zero and two holes, respectively. Cl ions then move strongly closer to Pt^{4+} atoms. As a result of this periodic lattice distortion, matrix elements for hopping from Pt^{4+} ions increase and holes gain energy by virtual hops from Pt^{4+} to Cl. This strong Peierls-distorted-disproportionation phase is well described as Cl–Pt^{4+}–Cl trimers, alternating with weakly coupled empty Pt^{2+} sites: the Pt^{4+}–Cl distance is 2.318 Å, and the Pt^{2+}–Cl distance is 3.085 Å. The electron–electron repulsion U at Pt sites is not sufficient to destroy the CDW phase or to significantly reduce its magnitude. Therefore, it is not necessary to explicitly include correlations as far as the magnitude of the CDW is concerned. Indeed, as shown in [2], one may introduce effective free-electron-model parameters that give correct values for the ground-state uniform Peierls distortion. However, calculations in [2], and our calculations below, show that it is necessary to introduce U if one wishes to describe *electronic* properties. The optical absorption of PtCl has two peaks, at

0953-8984/99/390415+08$30.00

approximately 2.5 eV and 5.5 eV, corresponding essentially to $Pt^{4+} \rightarrow Pt^{2+}$ and $Pt^{4+} \rightarrow Cl$ local charge-transfer excitons [2]. The width of the $Pt^{4+} \rightarrow Pt^{2+}$ band is of the order of 0.7 eV [4]. This corresponds to a tunnelling time of about 5.9×10^{-15} seconds for a hole to tunnel from one Pt^{2+} site to a near-neighbour one. Due to the large Peierls distortion, the inter-valence charge-transfer (IVCT) gap is large, $\approx$2.5 eV $= 2.9 \times 10^4$ K. The energy E_{ph} of the optical phonon with wave vector $k = 0$ in the system is 38 meV $= 437$ K. The period of a phonon oscillation is thus equal to 1.4×10^{-13} s.

Resonant Raman scattering (RRS) measurements on PtCl were reported in [1], and the observed strong red-shift of overtones interpreted convincingly in terms of multiphonon bound states, i.e., intrinsic local modes (ILMs). Below, we adopt a simple Brownian motion picture of a RRS event; see figure 1. We first consider the simplest and most probable scenario in the local (atomic) limit appropriate for PtCl. In the first stage, figure 1(a), a photon is absorbed, and a hole is transferred from a Pt^{4+} ion to the neighbouring Pt^{2+} ion, creating a pair of neighbouring Pt^{3+} ions. Then, in the simplest situation, after some time the hole recombines, emitting a photon. In more complicated and less probable scenarios a number of further hops (tunnelling steps) may occur before the recombination. Let us first consider the simplest scenario above. After a hole is transferred to the empty Pt site, the Cl ion between

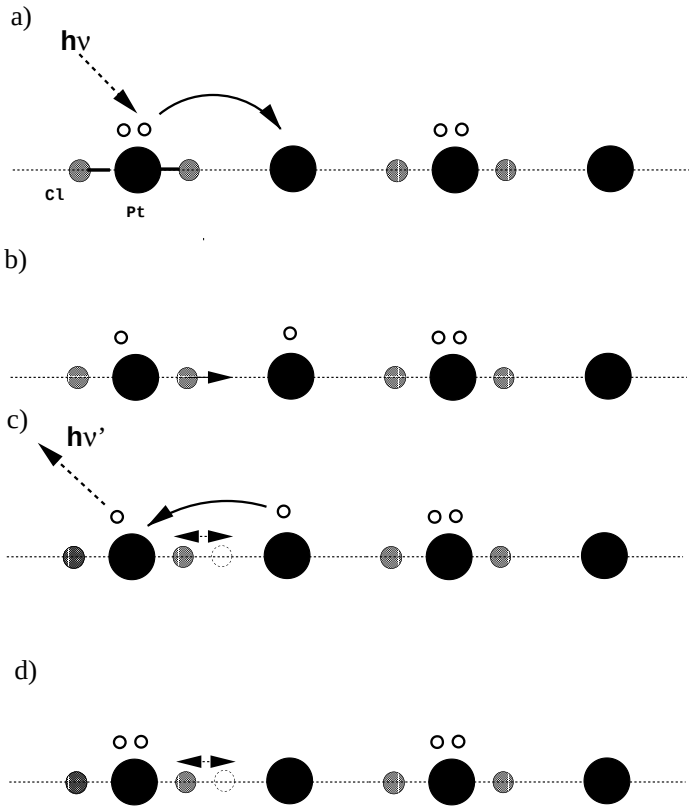

Figure 1. A simple picture of a resonant Raman scattering event in the localized (atomic) limit.

two Pt^{3+} sites is no longer at the minimum of its adiabatic energy. Therefore, it starts to move, transferring the electronic energy to the energy of the lattice; see figure 1(b). After some time the hole hops back and a photon is emitted; see figure 1(c). Some energy remains in the lattice vibration; see figure 1(d). This energy corresponds to a quantized intrinsic localized mode (ILM). The quantum ILM energy levels are then observed as peaks in the RRS spectrum [1]. Measurements in [1] also found small-magnitude ILM-plus-fundamental side-peaks. These correspond to more complicated situations, in which the dynamics of at least two neighbouring trimers are involved. One of the trimers is excited into an N-phonon state, and the other one is in a one-phonon state. The amplitude of the corresponding peaks is much less than the amplitude of pure ILM peaks [1]. This fact is readily explained in the local picture of a RRS event described above. The dynamics of two trimers may become excited by multiple-hop events. These multiple-hop events have much less probability than the event in figure 1, due to the very high degree of localization in PtCl because of its very strong charge disproportionation [1, 2]. An important issue is that of why, if two-trimer excitations do occur, they appear as $(N-1, 1)$ modes, such that there are $N-1$ phonons on one trimer, and one phonon on the other. Other possible modes, for instance $(N-2, 2)$ modes, are apparently not observed in the RRS spectrum within the experimental resolution [1]. The answer to this puzzle seems to lie in the bosonic nature of phonons. Bosons tend to bind together, or 'condense', into composite states. The expression for the probability amplitude for a boson branching to some quantum state has a multiplication factor $\sqrt{M+1}$, where M is the number of bosons already in this state. Therefore, if N phonons are emitted by an exciton and are allowed to branch into two states (in our case two neighbouring trimers), the most probable outcome is for all of them to go to the same trimer, and then the next most probable configuration is the $(N-1, 1)$ configuration. We reiterate that the validity of the whole picture described above is based upon the strongly localized nature [1] of PtCl, i.e., upon the fact that being at a particular trimer is close to being in a well defined quantum state. As noted above, the energy of the $k = 0$ optical phonon in PtCl is 437 K. Measurements [1] were performed on samples cooled to 12 K. Even allowing for some local heating of the sample by the laser light, it is impossible for the temperature of the sample during the measurements to become close to the thermal excitation threshold of optical phonons. Therefore, there cannot be thermalized optical phonons in the system. In spite of this, measurements [1] revealed clearly pronounced 'ILM-plus-fundamental' features. These features are anti-Stokes-like lines, corresponding to a transformation of a pre-existing optical phonon into an ILM by the absorption of a photon. This means that the system clearly has pre-existing optical phonons and is, therefore, not in thermal equilibrium. In order for such a non-equilibrium phenomenon to be possible, optical phonons must have a long lifetime; that is, the condition $\tau_{\text{phonon}} G \sim 1$ should be satisfied, where G is the number of photons absorbed in the sample per second per unit PtCl cell. A detailed study of this interesting phenomenon requires further experiments, particularly of the anti-Stokes component of the RRS spectrum. It is worthwhile noting that non-thermal phonon distributions in other strongly coupled electron–phonon materials (e.g. conjugated polymers and proteins [5–7]) have been invoked recently. Also the long, multi-timescale relaxation of *classical* ILMs has been observed in numerical simulations [8] on non-linear lattices.

The usual adiabatic parameter, which is the ratio of the characteristic phonon and electron frequencies, is small for PtCl. Therefore, the amplitude of the Peierls distortion should be well described in the adiabatic approximation. On the other hand, as was shown in [9], the purely adiabatic theory fails to describe the dynamic optical absorption attributed to breathers. This is related to the fact that, although the adiabatic approximation may describe well the amplitude of the wave function, it fails to correctly incorporate phase effects. The phase of the wave

function does not play a role if one is calculating the amplitude of the Peierls distortion, since this calculation seeks the minimum of the adiabatic energy and is phase insensitive. However, phase effects play a direct role in, e.g., the optical absorption, where effects of constructive and destructive interference are present. One goal of our work here was to check the limits of validity of the adiabatic approximation for the calculation of energies of quantum ILMs. Our conclusion is that, although the adiabatic approximation can work well for a calculation of the linear part of the energies, it may fail if one is calculating the non-linear corrections, which correspond to the binding energies of phonons in bound states. Since these binding energies are typically small, they may be strongly influenced by non-adiabatic effects.

A minimal phenomenological model for describing qualitative features of PtCl is the two-band Peierls–Hubbard model, introduced for this purpose in [2]. The ingredients of this model are the bond-length-dependent on-site energy difference between Pt and Cl orbitals, the bond-length-dependent hopping matrix element connecting Pt and Cl ions, and the Hubbard repulsion U for electrons on a Pt atom. Lattice degrees of freedom are described by the linear nearest-neighbour elastic spring constant K. Further studies [3] have shown that, since the Coulomb interaction at the length scale of one lattice constant is not fully screened, there is a need to take this interaction into account, assuming some reduced effective charges on neighbouring sites. The Hamiltonian of our model is

$$\begin{aligned} H = \sum_{l=-\infty,\sigma}^{\infty} & -t_0(1-\alpha\Delta_l)(c^+_{l,\sigma}c_{l+1,\sigma} + \text{h.c.}) + U\sum_{l=-\infty}^{\infty} n_{2l,\uparrow}n_{2l,\downarrow} \\ & + \sum_{l=-\infty}^{\infty}\left[\frac{K\Delta_l^2}{2} + \frac{P_l^2}{2m_l}\right] + \sum_{l=-\infty}^{\infty} V_c\frac{(n_l - Z_l)(n_{l+1} - Z_{l+1})}{R_{l,l+1}} \\ & - \sum_{l=-\infty}^{\infty}[-\epsilon + \beta(\Delta_{2l+1} + \Delta_{2l})]\,n_{2l}. \end{aligned} \tag{1}$$

Here c_i^+, c_i are electron creation and annihilation operators, t_0 is the Pt $\leftrightarrow$ Cl transition amplitude, α and β are the electron–phonon coupling strengths, Δ_l is the bond-length change for the lth bond, U is the electron repulsion at Pt sites, ϵ is the energy difference between Cl and Pt sites, K is the linear elastic constant, m_l is the mass of the lth atom, V_c is a phenomenological parameter related to the charge screening, and Z_l is the positive ion charge at the site l [3]. We assume Pt sites to take even indices. The filling is three electrons (or one hole) per unit cell. Calculations were performed on 12-site chains, using numerical exact diagonalization and the method of increments described in [10]. The lattice was treated adiabatically. The coupling constants were chosen to fit the experimental results for the magnitude of the Peierls distortion, the positions and magnitudes of the $Pt^{4+} \rightarrow Pt^{2+}$ and $Pt^{4+} \rightarrow$ Cl optical absorption peaks, and the optical phonon frequency. Then the non-linear adiabatic potential for Cl was calculated by fixing the Peierls-distorted positions of all sites except that of one Cl atom, and calculating the energy of the full system as a function of the position of this chosen Cl atom; see figure 2(a). The displacement X is measured with respect to the undistorted phase. Positive X means a displacement in the direction of the Pt^{2+} site. The minimum of the potential is at $X = -0.37$ Å, which is the value for the Peierls distortion. At $X = 0.17$ Å the calculated potential has a non-analytic point. At this point the first derivative of the potential with respect to X has a jump. Physically this non-analytic point corresponds to a transfer of a hole from the Pt^{4+} site to the closest Pt^{2+} site. The mechanism of this transfer is as follows. As X increases, the electron–phonon coupling leads to an energy increase at the Pt^{4+} site. Two holes at the Pt^{4+} site experience the Hubbard repulsion. At $X = 0.17$ Å the Hubbard repulsion dominates and one hole is transferred to the closest Pt^{2+} site. In this situation, the potential suddenly softens. This effect is related to the potential formation of

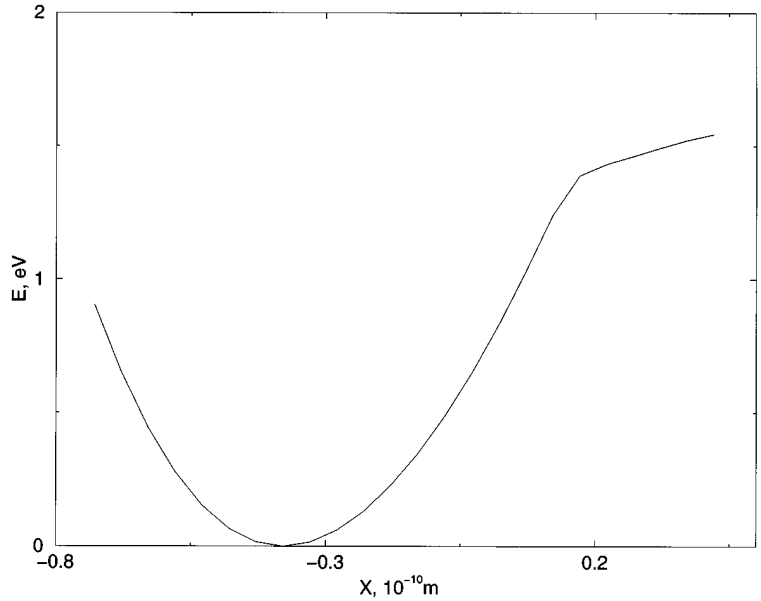

(a)

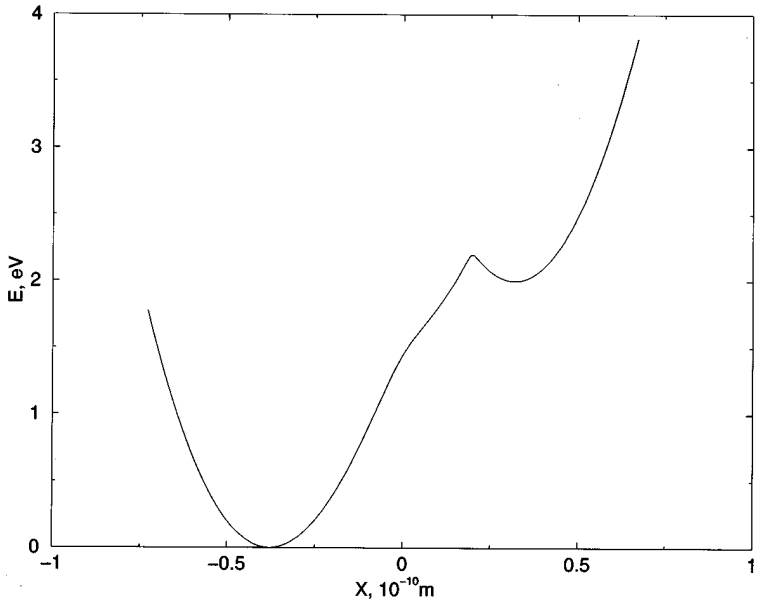

(b)

Figure 2. (a) The adiabatic potential for a single Cl atom. The zero of energy corresponds to the equilibrium position in the Peierls-distorted phase. X is the shift of the Cl atom, measured from the undistorted phase. (b) The adiabatic potential for two symmetrically displaced Cl atoms in one trimer.

local kink–antikink pairs in the system, which is illustrated in figure 2(b). In this figure we plot the adiabatic energy for *two* Cl atoms displaced symmetrically. We observe a local minimum

in the adiabatic energy, which should be attributed to the creation of a kink–antikink pair. Having the adiabatic potential, figure 2(a), non-linear corrections to quantum levels of a ^{37}Cl site oscillating in this potential may be accurately calculated using perturbation theory for a quantum anharmonic oscillator [11]. First we performed our calculations without the Coulomb term and found the non-linear softening of the potential to be seriously underestimated. We were not able to reproduce the experimental values for the non-linear corrections with any reasonable choice of model parameters. One can view this fact as a confirmation of the importance of intra-chain Coulomb interactions in PtCl [3]. We then added the Coulomb term and were able to fit the measured values of the non-linear corrections using the following set of model parameters: $t_0 = 0.75$ eV, $U = 2.44$ eV, $\beta = 1.77$ eV Å^{-1}, $\alpha = 3.55$ eV Å^{-1}, $\epsilon = 0.90$ eV, $K = 9.7$ eV Å^{-2}, $V_c = 8.18$ eV Å. Our value of the Hubbard U is close to $U = 2.0$ eV, obtained in [4] by quantum chemical configuration interaction calculations on a Cl–Pt–Cl cluster. This correspondence is reasonable, since the Hubbard U is characteristic of a highly localized d orbital, and should not change much when going from an atomic cluster to a crystal. The value of the Coulomb repulsion coefficient V_c has the same order of magnitude as the value 13.3 eV Å found in [3] using a Hartree–Fock approach. The adiabatic potential in figure 2(a) is quadratic near the equilibrium point and may be written as

$$E_{ad} = F_1\,\mathrm{d}x^2/2 + F_2\,\mathrm{d}x^3/3 + F_3\,\mathrm{d}x^4/4.$$

The quantum levels for the Cl atom moving in this potential well are then given by the approximate expression [11]

$$E_n = \hbar\omega\left[(n+1/2) + \left(\frac{\epsilon_1}{\hbar\omega}\right)^2 A_n^{(2)} + \frac{\epsilon_1}{\hbar\omega}B_n^{(1)} - \left(\frac{\epsilon_1}{\hbar\omega}\right)^2 B_n^{(2)}\right]. \tag{2}$$

Here

$$A_n^{(2)} = \frac{15}{4}\left(n^2+n+\frac{11}{30}\right)$$

$$B_n^{(1)} = \frac{3}{4}(2n^2+2n+1) \qquad B_n^{(2)} = \frac{1}{8}(34n^3+51n^2+59n+21)$$

$$\omega = \sqrt{F_1/2m} \qquad l = \sqrt{\hbar/m\omega}$$

$$\epsilon_1 = l^3F_2/3 \qquad \epsilon_2 = l^4F_3/4.$$

In figure 3 we have plotted the results for energy levels shifts, together with experimental RRS results for Pt^{37}Cl [1]. Here N is the number of phonons in the bound state. For small N we find good agreement with the experiment. At $N = 5$ the amplitude of the shift becomes larger than our estimates. This suggests an additional softening non-linearity in the system at sufficiently large amplitudes. It may be that this non-linearity is related to non-adiabatic effects, which become more important as the amplitude of the ILM increases.

To conclude, intrinsic localized modes (ILMs) in PtCl give an example of non-linear, thermally non-equilibrium excitations in crystal lattices. Similar phenomena, probably related to energy localization and non-thermalization, have been experimentally observed, especially via ultrafast spectroscopy, in several electron–phonon-coupled systems. These systems include polymers [5], glasses [6], and biological systems such as proteins [7]. The unique advantage of PtCl and related MX materials is that one can obtain very good crystals with a known structure and controllable and tunable non-linearity strengths. Therefore, PtCl provides an ideal opportunity for making quantitative models and testing theories of intrinsic non-linear energy localization (as well as extrinsic energy localization [12]). In this letter, a two-band Peierls–Hubbard model with screened Coulomb interaction, in the adiabatic approximation,

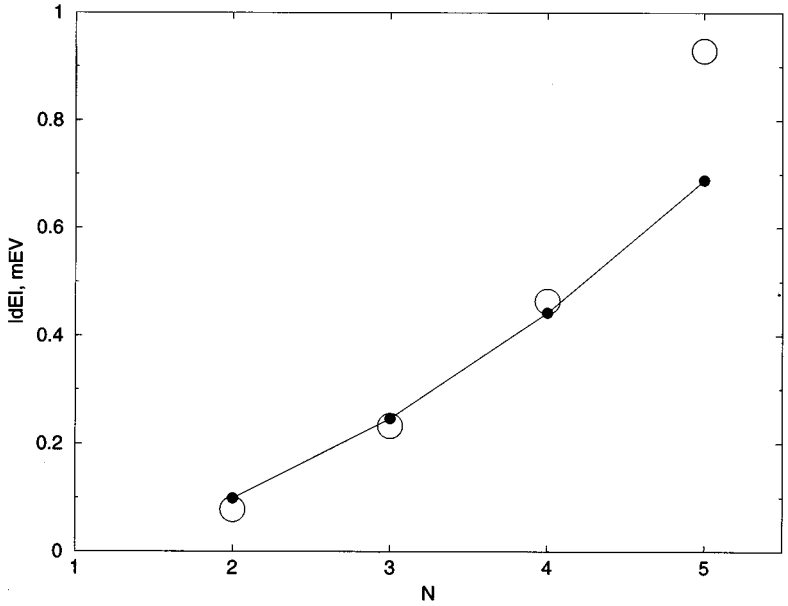

Figure 3. The absolute value of the non-linear energy level shift. Dots correspond to the theoretical prediction. Circles are the experimental results for $Pt^{37}Cl$ [1]; the size of a circle gives the experimental uncertainty due to the finite RRS peak width. Lines are guides to the eye.

has been applied to PtCl. We have found that this gives a good qualitative account of the main phenomena related to the existence of intrinsic localized modes in PtCl, at least for small numbers of bound quanta. We have also shown that the screened Coulomb interaction is a necessary ingredient within the adiabatic model for explaining the quantitative magnitude of non-linear shifts in the resonant Raman spectrum. We have observed that there exists an additional source of softening in the system at sufficiently large amplitudes. We suspect that this is related to non-adiabatic effects; future investigations will be focused on a quantitative theory of these effects. Other important directions for future experimental and theoretical research include measuring lifetimes of quantum ILMs, understanding the intrinsic mechanisms for their decay and their interactions with impurities, as well as studying photoexcited ILMs [13]. PtCl offers the first controlled experimental possibility to investigate these fundamental questions, with wide consequences for energy localization and transport in strongly correlated hard, soft, and biological electronic materials.

We are grateful for stimulating discussions with S Aubry, A Shreve, B Swanson and C R Willis. Work at Los Alamos is supported by the US DoE, under contract W-7405-ENG-36.

References

[1] Swanson B I, Brozik J A, Love S P, Strouse G F, Shreve A P, Bishop A R, Wang W Z and Salkola M I 1999 *Phys. Rev. Lett.* **82** 3288
[2] Tinka Gammel J T, Saxena A, Batistic I, Bishop A R and Phillpot S R 1992 *Phys. Rev.* B **45** 6408
[3] Batistic I, Huang X Z, Bishop A R and Saxena A 1993 *Phys. Rev.* B **48** 6065
[4] Wada Y, Mitani T, Toriumi K and Yamashita M 1989 *J. Phys. Soc. Japan* **58** 3013
[5] Lanzani G, Benner R E and Vardeny Z V 1997 *Solid State Commun.* **101** 295
[6] Gafert J, Pschierer H and Friedrich J 1995 *Phys. Rev. Lett.* **74** 3704

[7] Fritsch K, Friedrich J, Parak F and Skinner J L 1996 *Proc. Natl Acad. Sci. USA* **93** 15141
[8] See, e.g., Rasmussen K O, Aubry S, Bishop A R and Tsironis G P 1999 *LANL Preprint* patt-sol/9901002
[9] Horovitz B, Bishop A R and Phillpot S R 1988 *Phys. Rev. Lett.* **60** 2210
[10] Malek J, Kladko K and Flach S 1998 *JETP Lett.* **67** 1052
[11] Flugge S 1974 *Practical Quantum Mechanics* (Berlin: Springer)
[12] Love S P, Huckett S C, Worl L A, Frankcom T M, Ekberg S A and Swanson B I 1993 *Phys. Rev.* B **47** 1107
[13] Wang W Z, Bishop A R, Tinka Gammel J T and Silver R N 1998 *Phys. Rev. Lett.* **80** 3284